IMPACT CRATER ANALYSIS OF SOUTHCENTRAL ARABIA TERRA AND IMPLICATIONS FOR VOLATILES. M.E. Landis and N.G. Barlow, Department of Physics and Astronomy, Northern Arizona University, Flagstaff, AZ 86001-6010, USA (lel56@nau.edu, Nadine.Barlow@nau.edu)

Introduction: The Arabia Terra region of Mars is of interest because of its extensive cratering history and morphologies that have been linked to subsurface volatiles. The area of interest presented in this abstract is the subset of Arabia Terra from 0-20°N, 0-30°S that contains 1076 craters larger than 5-km-diameter and over 16,000 craters between 1- and 5-km diameter.

Arabia Terra's geologic history has included resurfacing events [1], present water enrichment [2], and indications south of the area that point to a salt water sea in the vicinity of the Opportunity landing site [3]. These factors make Arabia Terra a prime site to examine the history of surficial and subsurface volatiles through impact crater analysis.

Methodology: Impact craters ≥5-km-diameter in the study region were obtained from Barlow's revised *Catalog of Large Martian Impact Craters* and craters 1-5-km-diameter were added to the catalog using the Java Mission-planning and Analysis for Remote Sensing (JMARS) software. Morphology classification methods are described in [4]. A total of 71 craters between the diameters of 3- to 5-km were identified and added to the survey. Craters <3 km were not included in the depth analysis because of the effective MOLA resolution limit [ie 5]. Table 2 describes the results of the primary impact and modification morphologies.

Crater depths were calculated using a combination of Mars Orbiter Laser Altimeter (MOLA) and shadow length measurement techiques based on the diameter of the crater. Craters greater than the simple-to-complex transition ration (~7 km [6,7]) were calculated using the MOLA data application in JMARS. Craters between 3- and 5-km-diameter had depths calculated using both MOLA data and shadow length measurements. Equations for flat and parabolic floor configurations were used in the shadow length measurement calculations [8,9]. Orignal depths based on current crater diameters were calculated for craters >5-km-diameter.

Ages of crater morphologies were calculated using relative crater distributions in CraterStats2 [10]. Figure 1 shows the isochron for the entire study region, which is consistent with the Noachian age of Arabia Terra previously cited in the literature [11]. Ages of individual morphologies found in the study region are listed in Table 2.

Table 1- Morphologies included in the study are listed below along with the number of craters identified as each morphology as well as the percent of total craters each morphology represents.

Morphology		Number	% of total craters
Primary Impact	Central Pit	22	1.92%
	Central Peak	10	0.87%
	Nested Crater	5	0.44%
	Layered Ejecta	359	31.30%
Modification	Terrain Softening	14	1.22 %
	Inverted Crater	20	1.74%
	Ejecta blanket infilling	103	8.98%
	Scalloped/serrated rim	272	23.71%
Floor Deposits	Chaotic-type textures	85	7.41%
	Floor peaks	163	14.21%
	Sand dunes	78	6.80%
	Layered deposits	182	15.87%
	Floor pits	107	9.33%
	Lineated Floor Deposits	46	4.01%
	Floor ridges	151	13.16%
	Total with floor deposits	749	65.30%

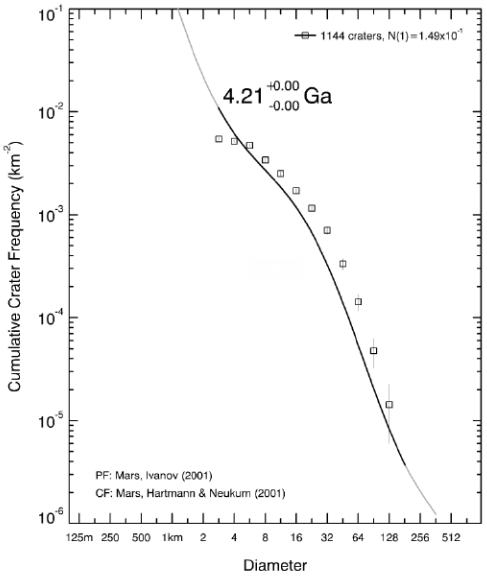

Figure 1-The CraterStats2 isochron for the relative crater count of Arabia Terra is shown above. The age based on the isochron fit is given in the figure for the entire study portion of Arabia Terra.

Table 2-Ages for each morphology type are listed. Ages were found using the relative crater disribution fitting program CraterStats2

Morphology		Age (Ga)
Study region		$4.21^{+0.00}_{-0.00}$
Primary Impact	Central Pit	$3.48^{+0.06}_{-0.11}$
	Central Peak	$2.92^{+0.38}_{-0.89}$
	Nested Crater	$1.48^{+0.66}_{-0.66}$
Modification	Terrain Softening	$1.89^{+0.56}_{-0.56}$
	Inverted Crater	$3.72^{+0.04}_{-0.05}$
	Scalloped/serrated rim	$4.03^{+0.01}_{-0.01}$
Floor Deposits	Chaotic-type textures	$3.93^{+0.02}_{-0.02}$
	Floor peaks	$3.98^{+0.01}_{-0.01}$
	Sand dunes	$3.92^{+0.02}_{-0.02}$
	Layered deposits	$3.99^{+0.01}_{-0.01}$
	Floor pits	$3.92^{+0.01}_{-0.02}$
	Lineated Floor Deposits	$3.77^{+0.03}_{-0.03}$
	Floor ridges	$3.90^{+0.01}_{-0.01}$

Results: Of the 1147 craters ≥5-km-diemeter, approximately 65% displayed at least one morphology type of interest. Morphologies that have been linked to subsurface volatiles like central pit craters [12] and terrain softening [13] are present in the region, indicating that surficial and subsurface volatiles have affected craters in the region. The size-frequency distribution as well as location present an opportunity to constrain the times and locations of volatiles in south central Arabia Terra.

Figure 2 shows the distribution of nested craters in the study region. Nested craters appear at mid-elevations in this region instead of at the lowest elevation that would be more consistent with a marine formation model [14]. One possible reason for this difference is that a resurfacing event at low elevations that has removed the nested craters at low elevations. Another is that a weaker layer of material, not necessailry emplaced in a marine environment, overlies the bedrock and the impact is more easily excavating through the upper material. The age for nested craters based on CraterStats2 analysis is 1.48±0.66 Ga, which is more recent that the other crater morphologies that are more consistent with a Late Heavy Bombardment age. However, only five nested craters have been identified in this portion of Arabia Terra, and including results from the entire region would expand the sample size and further constrain this age. The age of nested craters also can temporally limit the formation of the weak overlayer in the area.

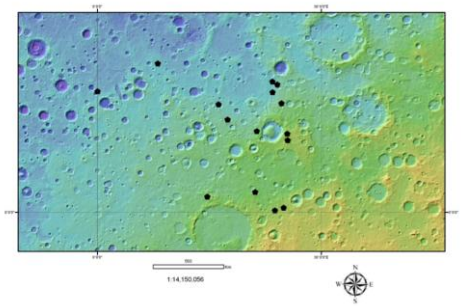

Figure 2- Distribtuion of nested craters in the study region of Arabia Terra is shown, with the MOLA background where blue indicates lower elevation and yellow/orange higher elevation.

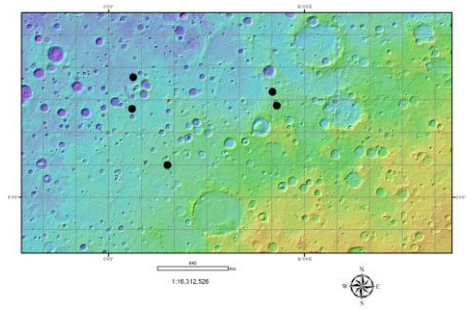

Figure 3-Distribution of high d/D craters within the study region of Arabia Terra.

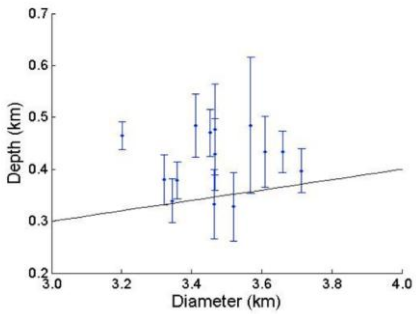

Figure 4- The depth-diameter ratio of fourteen craters 3-5km that display high d/D ratios. The black line shows the 1/10 d/D ratio.

We also found that cracters <5 km showed a high depth-diamter ratio (d/D). The distribution of 14 small craters that display a high d/D ratio are shown in Figure 3, with the d/D plot shown in Figure 4. The depth-diameter plot shows the shadow length measurement as a point with the error bars the difference between the shadow length measurement value and the MOLA value for the depth. The black line represents the 1/10 depth-diameter value.

The ages of crater morphologies in the study region of Arabia Terra generally date to the Late Heavy Bombardment period. Some crater morphologies that have <15 craters identified in the region give ages closer to 2 Ga than the 3-4 Ga age range for morphologies with more craters. Adding in data from the remaining regions in Arabia Terra will statistically improve these ages.

Conclusions: Morphologies that have formation models linked to subsurface volatiles are present in this region of Arabia Terra. These morphologies mostly give ages consistent with the Late Heavy Bombardment. Nested craters and high depth-diameter ratio craters indicate a weak surface layer in this portion of Arabia Terra.

Acknowledgements: This research is supported by NASA MDAP award NNX10AN82G to NGB.

References: [1] Hynek, B. M., and Phillips, R. J. (2001). *Geology*, 29, 407-410. [2] Boynton W. V. et al. (2002). *Science*, 297, 81-85. [3] Squyres S. W. et al. (2004). *Science*, 306, 1698-1703. [4] Landis M.E. and Barlow N.G. (2012). *LPSC XLIII*, abs. #1255. [5] Robbins, S. J. and B. M. Hynek, (2012). *3rd Planetary Crater Consortium*, abs. #1203. [6] Garvin J.B. et al. (2000). *Icarus*, 144, 329-352 [7] Garvin J.B. et al. (2003). *6th Intern. Conf. on Mars*, abs. #3277. [8] Pike, R. J. (1988). In *Mercury* (F. Vilas, C. R. Chapman, and M. S. Matthews, eds.), UAz Press, 165-273. [9] Chappelow, J. E., Sharpton, V. L. (2002). *MAPS*, 37, 479-486. [10] Michael G.G., et al. (2010). *EPS Letters*. [11] Werner, S. C. and Tanaka, K. L. (2011). *Icarus*, 215, 603-607. [12] Barlow N.G (2010), *GSA SP 465*, 15-27. [13] Squyres S.W. and M.H. Carr (1986), *Science*, 231, 249-252. [14] Ormó J. et al. (2004). *MAPS*, 39, 333-346.